ARCHIVES OF MECHANICS
Arch. Mech. **78** (3), 261–282, 2026, https://doi.org/10.24423/aom.4932

Analytical and numerical analysis of a continuous model of a flexible suspension element under vertical loads

I. RUDKO[1*], B. BAKAY[1],
V. LOVEIKIN[2], Y. ROMASEVYCH[2]

[1] *Department of Agricultural and Forest Engineering, Ukrainian National Forestry University, 103 General Chuprynka St, Lviv 79057, Ukraine, e-mail[*]: ihor.rudko@nltu.edu.ua (corresponding author)*

[2] *Department of Machines and Equipment Design, National University of Life and Environmental Sciences of Ukraine, 12 Heroiv Oborony, Kyiv 03041, Ukraine*

Conducting static analysis to determine operational characteristics of a flexible element is a crucial stage in the design of suspension engineering structures. Considering the structural features and production requirements for computational accuracy, the use of theoretical foundations of the catenary method is adopted as a rational approach for the static analysis of suspension systems. Based on the principles of the developed algorithm and the proposed approach to modelling and calculating suspension structures, the geometric and force parameters of a supporting element, positioned within a single span and loaded by the combined action of uniformly distributed and concentrated vertical loads, have been determined. The parameters of the supporting element were established by constructing and solving systems of transcendental equations. Due to the lack of widely used modern software complexes that would allow researchers to solve systems of this type of equations, this paper demonstrates that the required results can be obtained by employing specialized computer software (using the method of successive approximations with a predefined accuracy, which minimizes the amount of work and time required) or by using computational algorithms of spreadsheet processors (applying the graphical-analytical method, which is labour-intensive but allows for the establishment of the uniqueness of the problem's solution). The paper presents schematic diagrams illustrating the vertical load, tensions, and sag of the supporting element, along with the results of numerical modelling (illustrated by a specific example).

Key words: flexible element, suspension structure, combined vertical loading, tension, deflection.

1. Introduction

Suspension engineering structures are complex technical systems that, alongside their supporting elements, comprise supports, special equipment, fastenings, and other components. To evaluate the effectiveness of such systems in construction practice, a number of indicators are used and technical tasks are formulated, primarily related to the need to minimise metal consumption (energy intensity), increase reliability (fault tolerance, durability), optimise operating parameters (loads, dimensions, mass, accuracy of functioning, etc.). As a result, due to the increasing complexity of suspension structures and the rising requirements for their operational efficiency (in some cases, the technical operation of supporting elements with minimal safety factors $n_{sk} \approx 2 \ldots 3$ [1], etc.), there is a need to optimise the functioning of component parts [2], rationally distribute loads in adjacent nodes, assess safety factors, and justify rational modes of operational processes [3, 4]. In the context of solving problems related to these issues, it is important to conduct a detailed structural analysis of suspension structures, as well as to justify the shape of sag curves and determine the main geometric characteristics and force parameters of flexible supporting elements as their main components (taking into account the structures' own weight, the magnitude of the payload, and other factors [5, 6]).

Currently, various methods are applied in engineering practice for calculating the operational parameters of flexible elements in suspension structures (depending on the established requirements for the complexity and accuracy of mathematical models, and the labour intensity of calculations). One of the universal and generally accepted methods for the numerical solution of problems in applied mechanics, specifically for calculating the design or operational parameters of flexible elements in suspended engineering structures, is the finite element method. When employing this method and defining the format of finite elements for structural components, a number of simplifications and approximations are typically adopted [7, 8]. In addition, it is important to perform high-quality discretization and on proper a posteriori error control, especially in places where the geometry (curvature) of the flexible element changes, which requires the researcher to have high professional training and practical skills in designing suspension systems.

Analytical methods for calculating suspension systems are somewhat more accurate in this regard. For solving certain specific problems in civil engineering and mechanical engineering, it is possible to apply analytical methods that consider a discrete model of the supporting element (which allows for the development of engineering calculation methodologies suitable for practical use under specific conditions). However, in general, compared to a discrete model, a continuous model of a flexible element is more universal and accurate.

The most widely approved analytical method for calculating suspension systems in industrial practice is the parabolic method [5]. However, according to the theoretical principles of this method, it is assumed that self-weight and other loads are uniformly distributed along the span length, and not along the length of the sag curve of the loaded suspension structure. Therefore, the parabolic method is generally a sufficiently approximate calculation method and can be applied in industrial practice either for determining the parameters of suspension system elements with small sags, or with a more or less uniform load distribution along the span length.

A significantly less approved analytical method for calculating suspended engineering structures is the catenary method (due to the complexity of constructing mathematical models and solving applied problems). However, this method is the most accurate in terms of reflecting the sag shape, determining the geometric characteristics and force parameters of the suspended flexible element [9, 10], and allows for the consideration of other additional factors when necessary (e.g., temperature and elastic deformations [11], support flexibility [3], an increase in the number of spans [6, 12], etc.).

In the context of parametric design and optimization of suspended engineering structures, analytical approaches based on perturbations are extremely relevant. In particular, perturbation methods based on the assumption of cable shallowness have been proposed to achieve fully analytical – although asymptotically approximate – solutions for the static problem of elastically extensible cables under general loads [13, 14], as well as for the catenary configuration functions and the equivalent stiffness matrix of inclined inextensible cables under self-weight [15]. The article [13] examines the mechanical properties of a cable for various orders of the perturbation scheme; it implements the perturbation method to solve the static problem of an inclined, shallowly submerged elastic cable under general three-dimensional loads, and compares the asymptotic results with the exact (numerical) results. The research paper [14] examines a static problem for elastic cables with slight sag, suspended at points at different levels under the influence of general vertical loads. With the aim of obtaining simple asymptotic expressions with the desired degree of accuracy, a perturbation method has been developed and exact equations have been formulated that describe the static problem for an elastic sagging cable (determining its displacements and tensions under the action of vertical static forces). In [15], by developing a two-stage perturbation scheme, an asymptotic formulation of the problem of statically indeterminate equilibrium was established, asymptotic solutions were obtained in the form of convergent polynomial series, and asymptotic descriptions were determined for the configuration of the chain line formed by inclined inextensible cables. The paper [16] presents an original hierarchical variant of the force method, based on the systematic application of asymptotic perturbation theories; it also examines problems of static equilibrium for inextensible shallow cables and derives analytical solutions in the form of parametric functions of geometric and inertial data. In the article [17], asymptotic closed-form solutions are proposed for the modal properties of cables with small deflections, taking into account their bending stiffness, tensile stiffness and torsional flexibility at supports; practical recommendations are formulated for the effective monitoring of cable structures for which the above-mentioned parameters are of significant importance.

Also for both stationary suspension systems and for engineering structures utilising moving components (ropes, carriages, loads, etc.), static analysis is fundamental or basic for their design [18–20].

2. Problem geometry and analysis

To conduct a static analysis of an engineering structure loaded with uniformly distributed and concentrated vertical loads, the developed algorithm and proposed approach to modelling and calculating the geometric characteristics and force parameters of supporting elements of suspension systems, as specified in [22], are utilised.

At the initial stage of the analytical and numerical analysis of the continuous model of a flexible suspension element, factors such as, for example, thermal and elastic deformations, support compliance, an increase in the number of spans, lateral and non-uniformly distributed loads, etc.) are not taken into account, as their influence varies from case to case and may be linear or non-linear [21], as well as constant or dependent on other factors [3]. Since, in the first stage of the calculations, we assume the flexible element to be perfectly rigid in tension, the problem considers flexible elements with a length of at least $L > \ell/\cos\alpha$ with small ($f_{\max} \leq 1/18\ell$) and large ($f_{\max} > 1/18\ell$) deflections [17].

For this purpose, within the established assumptions, the magnitudes of forces and the sag shape of the supporting element with length L, which is fixed at points A and B, and is in equilibrium when loaded at a point C with abscissa X_c by a concentrated force G, directed vertically downwards (Fig. 1), is determined in characteristic sections.

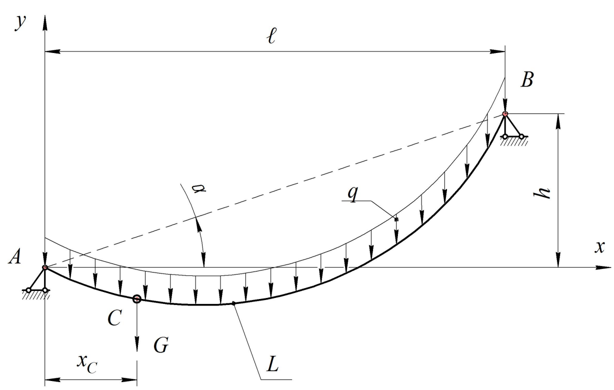

Fig. 1. Schematic diagram of the loaded supporting element in a rectangular coordinate system with the origin at the lower support.

The length of the supporting element section AC is equal to L_1, and the section CB is L_2. Since these sections of the supporting element are loaded with uniformly distributed vertical forces along their length, each of them coincides with a segment of the corresponding catenary [2, 7, 12], the equations can be written as follows (the first equation corresponds to the supporting element section AC, and the second to the section CB):

$$y_{/} = C_{1/} \cdot \cosh \frac{x - C_{2/}}{C_{1/}} - C_{3/}, \quad y_{//} = C_{1//} \cdot \cosh \frac{x - C_{2//}}{C_{1//}} - C_{3//}, \tag{2.1}$$

where $C_{1/(//)}$ are the parameters, and $C_{2/(//)}$ and $C_{3/(//)}$ are the coefficients of the catenaries (corresponding to $y_{/}$ and $y_{//}$ respectively) [m].

According to the presented scheme (Fig. 1), each characteristic section of the supporting element (AC and CB) corresponds to its own horizontal component $H_{/(//)}$ of its tension T:

$$C_{1/} = \frac{H_{/}}{q}, \quad C_{1//} = \frac{H_{//}}{q}, \tag{2.2}$$

where q is the intensity of the vertical load uniformly distributed along the curve (self-weight of structures, etc.) [N/m].

In accordance with the developed algorithm [22], the main equations for determining the six unknown coefficients $C_{i/(//)}$ (where $i = 1, 2, 3$) are constructed. First, two equations are obtained from the conditions of fixing the ends of the supporting element at points A and B (Fig. 1):

$$y_{/}(0) = 0, \qquad \cosh \frac{C_{2/}}{C_{1/}} = \frac{C_{3/}}{C_{1/}}, \tag{2.3}$$

$$y_{//}(\ell) = \ell \cdot \tan \alpha, \quad \cosh \frac{\ell - C_{2//}}{C_{1//}} = \frac{\ell \cdot \tan \alpha + C_{3//}}{C_{1//}}. \tag{2.4}$$

Also, one equation is obtained from the condition of continuity of the supporting element at the point C:

$$\begin{gathered} y_{/}(x_C) = y_{//}(x_C), \\ C_{1/} \cdot \cosh \frac{x_C - C_{2/}}{C_{1/}} - C_{3/} = C_{1//} \cdot \cosh \frac{x_C - C_{2//}}{C_{1//}} - C_{3//}. \end{gathered} \tag{2.5}$$

Considering the equilibrium of the supporting element at the point C, two more equations are obtained. In general, three forces act at this cross-section: the concentrated vertical force G, the reaction force of the right part of the supporting element $T_{C//}$, equal to its tension at this point, and the reaction

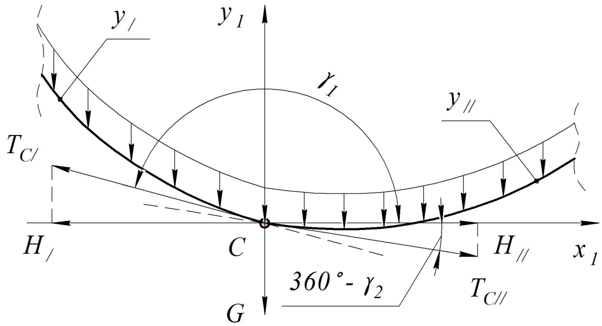

FIG. 2. Schematic diagram of the action of forces (tensions of the supporting element) at the point of its loading (with abscissa $x = x_C$) by concentrated force G (point C).

force of the left part of the supporting element $T_{C/}$, equal in magnitude to its tension at the point C and directed in the opposite direction (Fig. 2).

Projecting the forces applied at the point C onto the axes of the rectangular coordinates x_1 and y_1 ($x_1//x, x_1//x$, Figs. 1 and 2), the following equations of statics are obtained:

$$\begin{cases} T_{C/} \cdot \cos\gamma_1 + T_{C//} \cdot \cos\gamma_2 = 0, \\ T_{C/} \cdot \sin\gamma_1 + T_{C//} \cdot \sin\gamma_2 - G = 0, \end{cases} \tag{2.6}$$

where γ_1 and γ_2 are the angles between the tangents to the corresponding catenaries ($y_/$ and $y_{//}$) and the x-axis at point C (Fig. 2).

Given that $t_{C/} = -\frac{h_/}{\cos\gamma_1}$ and $t_{C//} = \frac{h_{//}}{\cos\gamma_2}$, it can be asserted, according to the first equation of the system (2.6), that the horizontal components of the supporting element's tension are equal in both characteristic sections ($H_/ = H_{//} = H$) [10, 12]. Furthermore, the equality of the catenary parameters $y_/$ and $y_{//}$ is asserted according to Eqs. (2.2), that is

$$C_{1/} = C_{1//}. \tag{2.7}$$

The second equation of the system of Eqs. (2.6) in this case takes the form

$$-H \cdot \tan\gamma_1 + H \cdot \tan\gamma_2 - G = 0. \tag{2.8}$$

Considering that the value of the derivative $y'_{/(//)}(x)$ at a given value of the argument x is equal to the tangent of the angle formed with the positive direction of the x-axis by the tangent to the graph of the function $y_{/(//)}(x)$ at the corresponding point $C(x_C, y_C)$, the following is obtained:

$$\begin{cases} \tan\gamma_1 = y'_{/}(x_C) = \sinh \dfrac{x_C - C_{2/}}{C_{1/}}, \\ \tan\gamma_2 = y'_{//}(x_C) = \sinh \dfrac{x_C - C_{2//}}{C_{1//}}, \end{cases} \tag{2.9}$$

$$\sinh \frac{x_C - C_{2//}}{C_{1//}} - \sinh \frac{x_C - C_{2/}}{C_{1/}} = \frac{G}{H}. \tag{2.10}$$

To construct the last transcendental equation, the length of the supporting element L is expressed in terms of the sought-after quantities, by dividing the integration interval $(0;\ell)$ into two sections: $(0;x_C)$ and $(x_C;\ell)$. In this case, the total length of the sag curve of the supporting element in sections and (Fig. 1) is

$$\begin{aligned} L = L_{AC} + L_{CB} &= \int_0^{x_C} \sqrt{1 + (y'_{/})^2}\, dx + \int_{x_C}^{\ell} \sqrt{1 + (y'_{//})^2}\, dx \\ &= C_{1/} \cdot \left(\sinh \frac{x_C - C_{2/}}{C_{1/}} + \sinh \frac{C_{2/}}{C_{1/}} \right) \\ &\quad + C_{1//} \cdot \left(\sinh \frac{\ell - C_{2//}}{C_{1//}} - \sinh \frac{x_C - C_{2//}}{C_{1//}} \right). \end{aligned} \tag{2.11}$$

In general, the constructed Eqs. (2.3)–(2.5), (2.7), (2.10) and (2.11) form a system of six transcendental equations, which contains six unknown coefficients (parameters) of the catenaries $C_{i/(//)}$ $(i = 1, 2, 3)$.

Currently, modern software complexes that would allow researchers to efficiently solve systems of transcendental equations of this type are not widely available. Therefore, to obtain the necessary results in an operational mode, it is advisable to develop and use specialised applied computer programs [23] that ensure minimal labour and time costs due to the use of the successive approximation method with a predefined (required) calculation accuracy.

If researchers do not have the opportunity to use specialised applied computer software, to obtain the necessary results (without loss of calculation accuracy), it is advisable to use computational algorithms of spreadsheet processors with the application of the graphical-analytical method. This method is relatively labour-intensive, but within the established limits of tension and sag of the flexible supporting element, it allows establishing the uniqueness of the problem's solution (the maximum tension of the supporting element is usually limited by its breaking force, taking into account the normative safety factor of the engineering structure, and the maximum sag is limited by the geometric characteristics of the supporting element's suspension scheme).

Therefore, in accordance with the basic principles of the graphical-analytical method for solving systems of transcendental equations of this type [22], and as a result of mathematical transformations, the specified system of equations can be reduced to a system of three equations (correspondingly, with three unknown coefficients).

$$
\begin{cases}
\sinh \dfrac{x_C - C_{2//}}{C_{1/}} - \sinh \dfrac{x_C - C_{2/}}{C_{1/}} = \dfrac{G}{H}, \\
\sinh \dfrac{x_C - C_{2/}}{C_{1/}} + \sinh \dfrac{C_{2/}}{C_{1/}} + \sinh \dfrac{\ell - C_{2//}}{C_{1/}} - \sinh \frac{x_C - C_{2//}}{C_{1/}} = \dfrac{L}{C_1^{/}}, \\
\cosh \dfrac{x_C - C_{2/}}{C_{1/}} - \cosh \dfrac{C_{2/}}{C_{1/}} - \cosh \dfrac{x_C - C_{2//}}{C_{1/}} + \cosh \dfrac{\ell - C_{2//}}{C_{1/}} = \dfrac{h}{C_{1/}},
\end{cases}
\tag{2.12}
$$

where h is the elevation difference between adjacent supports of the suspension structure [m]; $h = \ell \cdot \tan\alpha$ (Fig. 1).

To reduce the system of Eqs. (2.12) to a single transcendental equation (with respect to one unknown coefficient), pairwise addition and subtraction operations are performed in the last two equations of the system.

$$
\begin{cases}
\sinh \dfrac{x_C}{2C_{1/}} \cdot \cosh \dfrac{x_C - 2C_{2/}}{2C_{1/}} + \sinh \dfrac{\ell - x_C}{2C_{1/}} \cdot \cosh \dfrac{\ell + x_C - 2C_{2//}}{2C_{1/}} = \dfrac{L}{2C_{1/}}, \\
\sinh \dfrac{x_C}{2C_{1/}} \cdot \sinh \dfrac{x_C - 2C_{2/}}{2C_{1/}} + \sinh \dfrac{\ell + x_C - 2C_{2//}}{2C_{1/}} \cdot \sinh \dfrac{\ell - x_C}{2C_{1/}} = \dfrac{h}{2C_{1/}}.
\end{cases}
\tag{2.13}
$$

Also, the left and right sides of the equations in the system (2.13) are pairwise added and subtracted.

$$
\begin{cases}
\sinh \dfrac{x_C}{2C_{1/}} \cdot \left(\cosh \dfrac{x_C - 2C_{2/}}{2C_{1/}} + \sinh \dfrac{x_C - 2C_{2/}}{2C_{1/}}\right) \\
\quad + \sinh \dfrac{\ell - x_C}{2C_{1/}} \cdot \left(\cosh \dfrac{\ell + x_C - 2C_{2//}}{2C_{1/}} + \sinh \dfrac{\ell + x_C - 2C_{2//}}{2C_{1/}}\right) = \dfrac{L + h}{2C_{1/}}, \\
\sinh \dfrac{x_C}{2C_{1/}} \cdot \left(\cosh \dfrac{x_C - 2C_{2/}}{2C_{1/}} - \sinh \dfrac{x_C - 2C_{2/}}{2C_{1/}}\right) \\
\quad + \sinh \dfrac{\ell - x_C}{2C_{1/}} \cdot \left(\cosh \dfrac{\ell + x_C - 2C_{2//}}{2C_{1/}} - \sinh \dfrac{\ell + x_C - 2C_{2//}}{2C_{1/}}\right) = \dfrac{L - h}{2C_{1/}}.
\end{cases}
\tag{2.14}
$$

The necessary transformations of the equations in the system (2.14) are performed:

$$
\begin{cases}
\sinh \dfrac{x_C}{2C_{1/}} \cdot e^{\frac{x_C - 2C_{2/}}{2C_{1/}}} + \sinh \dfrac{\ell - x_C}{2C_{1/}} \cdot e^{\frac{\ell + x_C - 2C_{2//}}{2C_{1/}}} = \dfrac{L + h}{2C_{1/}}, \\
\sinh \dfrac{x_C}{2C_{1/}} \cdot e^{-\frac{x_C - 2C_{2/}}{2C_{1/}}} + \sinh \dfrac{\ell - x_C}{2C_{1/}} \cdot e^{-\frac{\ell + x_C - 2C_{2//}}{2C_{1/}}} = \dfrac{L - h}{2C_{1/}}.
\end{cases}
\tag{2.15}
$$

To simplify the calculation process, the following notations are introduced, and the conditions based on the physical meaning of the given problem are written:

$$\text{(2.16)}\qquad \begin{cases} X = e^{\frac{x_C - 2C_{2/}}{2C_{1/}}}, & Y = e^{\frac{\ell + x_C - 2C_{2//}}{2C_{1/}}}, \\ Z = \dfrac{L+h}{2C_{1/}} > 0, & V = \dfrac{L-h}{2C_{1/}} > 0, \\ K = \dfrac{x_C}{2C_{1/}}, & P = \dfrac{\ell - x_C}{2C_{1/}}. \end{cases}$$

In this case, the system of Eqs. (2.15) takes the form:

$$\text{(2.17)}\qquad \begin{cases} \sinh K \cdot X + \sinh P \cdot Y = Z, \\ \sinh K \cdot X^{-1} + \sinh P \cdot Y^{-1} = V. \end{cases}$$

Having determined X from the first equation and substituted it into the second equation of the system (2.17), the corresponding terms are grouped

$$\text{(2.18)}\qquad V \cdot \sinh P \cdot Y^2 + (\sinh^2 K - \sinh^2 P - Z \cdot V) \cdot Y + Z \cdot \sinh P = 0.$$

The solution of this quadratic equation with respect to the sought-after value Y is written

$$\text{(2.19)}\qquad Y_{1,2} = \frac{-\sinh^2 K + \sinh^2 P + Z \cdot V}{2V \cdot \sinh P} \pm \frac{\sqrt{(\sinh^2 K - \sinh^2 P - Z \cdot V)^2 - 4Z \cdot V \cdot \sinh^2 P}}{2V \cdot \sinh P}.$$

Thus, according to the second and first equations of the system (2.16), the following is obtained:

$$\text{(2.20)}\qquad \begin{cases} C_{2//} = \dfrac{\ell}{2} + \dfrac{x_C}{2} - C_{1/} \cdot \ln Y_{1,2}, \\ C_{2/} = \dfrac{x_C}{2} - C_{1/} \cdot \ln X_{1,2}. \end{cases}$$

Substituting the values (2.19) into the first Eq. (2.20), the formula for determining the sought-after parameter is obtained

$$\text{(2.21)}\qquad C_{2//} = \frac{\ell}{2} + \frac{x_C}{2} - C_{1/} \cdot \ln\left(\frac{-\sinh^2 K + \sinh^2 P + Z \cdot V}{2V \cdot \sinh P} \pm \right. \\ \left. \pm \frac{\sqrt{(\sinh^2 K - \sinh^2 P - Z \cdot V)^2 - 4Z \cdot V \cdot \sinh^2 P}}{2V \cdot \sinh P} \right).$$

Having established the dependencies $C_{2//} = f(C_{1/})$ (Eq. (2.21)) and $C_{2/} = f(C_{1/})$ (the second equation of the system (2.20) considering the first equation of the system (2.17)), they are substituted into the first equation of the system (2.12). As a result, a reduced transcendental equation is obtained with respect to one unknown variable (parameter $C_{1/}$), which is solved using the method of successive approximations or the graphical-analytical method. The remaining coefficients of the catenaries are determined from the equations constructed for this suspension structure (2.3)–(2.5), (2.7), (2.10) and (2.11).

The magnitude of the sag, measured from the chord of the span AB, at any point of the curved sections of the supporting element is determined using the following relationship (the lower index $_{/}$ applies when $0 \le x \le x_C$, index $_{//}$ when $x_C < x \le \ell$)

$$f = x \cdot \tan\alpha - C_{1/(//)} \cdot \cosh \frac{x - C_{2/(//)}}{C_{1/(//)}} + C_{3/(//)}. \tag{2.22}$$

To determine the abscissa x^* at which the sag of the supporting element reaches its maximum, the first derivative of the specified function is equated to zero.

$$\frac{df}{dx} = \tan\alpha - \sinh \frac{x^*_{/(//)} - C_{2/(//)}}{C_{1/(//)}} = 0. \tag{2.23}$$

From the given equality, $x^*_{/(//)}$ is determined

$$x^*_{/(//)} = C_{2/(//)} + C_{1/(//)} \cdot \operatorname{Arsinh}(\tan\alpha). \tag{2.24}$$

If $x^*_{/(//)} \in (0;\ell)$, then $x^* = x^*_{/(//)}$, otherwise $x^* = x_C$. The value of $f_{\max}$ is subsequently calculated according to formula (2.22) at $x = x^*$.

Using the formula for calculating the tension of the supporting element $T = H \cdot \cosh \frac{x}{C_1}$ at its arbitrary point, horizontally distant from the vertex of the catenary by a distance x [5, 22], its tensions in characteristic sections for each of the sections (Fig. 3) and the corresponding average tensions of the supporting element are determined.

Specifically, for the section of the supporting element AC (Fig. 4):

$$\begin{cases} T_A = H_{/} \cdot \cosh \dfrac{C_{2/}}{C_{1/}}, \\ T_{C\,left} = H_{/} \cdot \cosh \dfrac{C_{2/} - x_C}{C_{1/}}, \\ T_{av/} = \dfrac{1}{x_C} \displaystyle\int_{C_{2/} - x_C}^{C_{2/}} T(x)\,dx = \dfrac{H_{/}^2}{x_C \cdot q} \cdot \left(\sinh \dfrac{C_{2/}}{C_{1/}} - \sinh \dfrac{C_{2/} - x_C}{C_{1/}} \right), \end{cases} \tag{2.25}$$

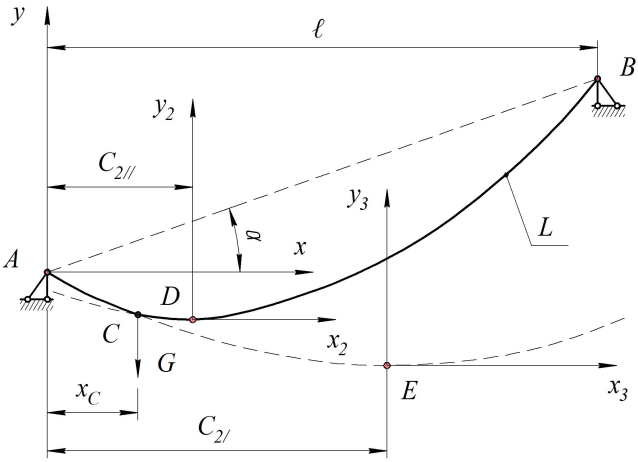

FIG. 3. Geometric parameters of the supporting element suspension scheme ($x_3//x_2//x, y_3//y_2//y$).

as well as for the section of the supporting element CB:

$$\begin{cases} T_{C\,right} = H_{//} \cdot \cosh \dfrac{C_{2//} - x_C}{C_{1//}}, \\ T_B = H_{//} \cdot \cosh \dfrac{\ell - C_{2//}}{C_{1//}}, \\ T_{av//} = \dfrac{1}{\ell - x_C} \displaystyle\int\limits_{x_C - C_{2//}}^{\ell - C_{2//}} T(x)\, dx \\ \qquad = \frac{H_{//}^2}{(\ell - x_C)\cdot q} \cdot \left(\sinh \dfrac{\ell - C_{2//}}{C_{1//}} - \sinh \dfrac{x_C - C_{2//}}{C_{1//}} \right). \end{cases} \tag{2.26}$$

The averaged value of the tension of the supporting element for both characteristic sections (within the entire span) is

$$T_{av} = \frac{x_C \cdot T_{av/} + (\ell - x_C) \cdot T_{av//}}{\ell}. \tag{2.27}$$

For researchers of suspension structures and engineers, it is important not only to be able to calculate the geometric characteristics and force parameters of the loaded supporting element at nodal points, but also to establish the nature of the distribution of loads, tensions, and deflections of the supporting element along the span length. Therefore, in order to ensure the practical application of the aforementioned theoretical principles during engineering calculations, in accordance with the obtained relationships, the horizontal distribution of vertical

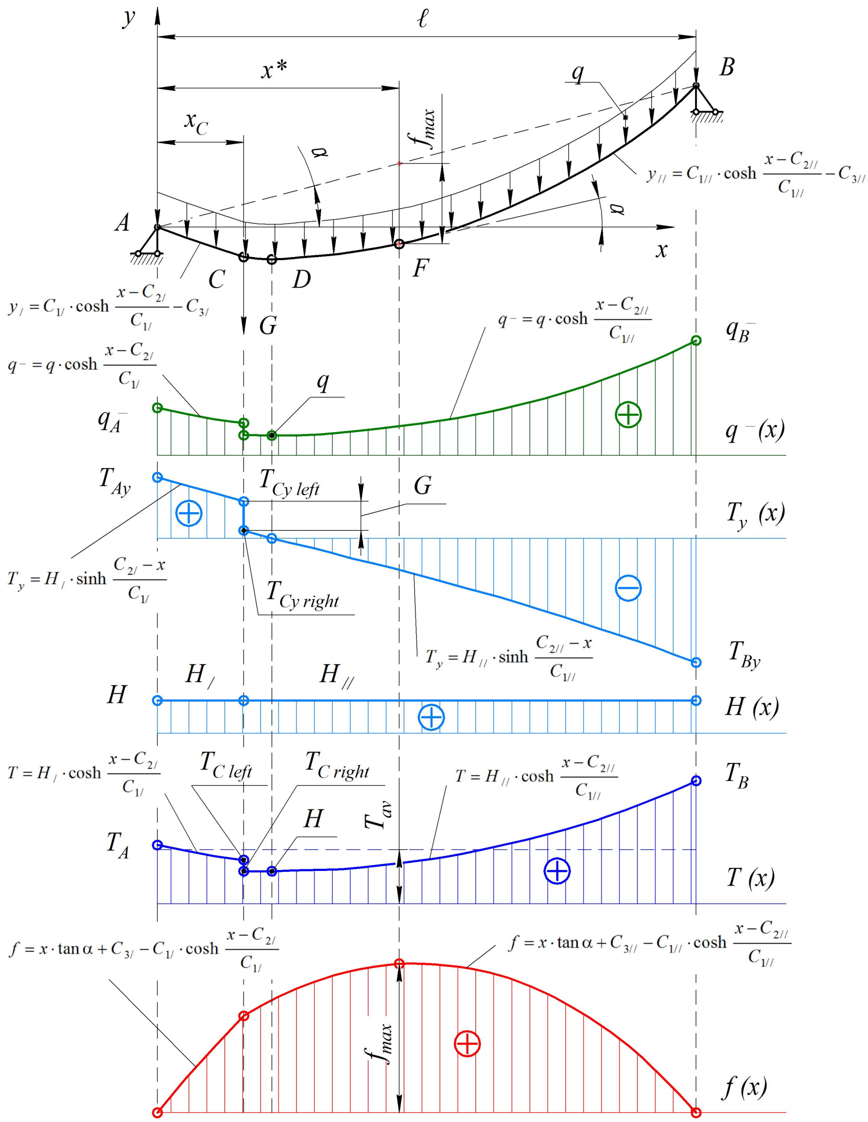

FIG. 4. Schematic representation of the diagrams of horizontal distribution of vertical load $q^{-}(x)$, tensions $T_y(x)$, $H(x)$, $T(x)$ and sag $f(x)$ of the supporting element along the span of the suspension structure.

load $q^{-}(x)$, tensions $T_y(x)$, $H(x)$ and $T(x)$, as well as the deflection of the supporting element $f(x)$, are graphically represented along the span length (Fig. 4).

In the diagram (Fig. 4), positive and negative values of the vertical component of the supporting element tension $T_y(x)$ are shown according to the rule, as for the shear force in a beam section (the force is considered positive if the resultant of external forces to the left of the section is directed upwards, and to the right – vice versa; in the opposite case, the shear force is considered negative). The obtained distribution of tensions in the supporting element (Fig. 4) is confirmed by the long-term practice of operating suspended engineering structures with vertical loading, particularly by the intensity of breakages and increased wear of the supporting elements precisely in the area of the upper supports – from the uphill side (breakages of supporting elements at the points of concentrated load application, particularly in the middle of the span, are extremely rare [3]).

3. Numerical modelling results (examples)

For the purpose of numerical static analysis of the suspension structure, in accordance with the proposed analytical dependencies, a single-span system is considered with the following geometric characteristics and vertical loading: $\ell = 300$ m, $\alpha = 20°$, $q = 28.65$ N/m, $L = 350$ m, $x_C = 50$ m, $G = 2000$ N.

First, the solution of the first equation of the system (2.12) concerning the parameter $C_{1/}$ is determined, using the computational algorithms of a spreadsheet processor (graphical-analytical method) and considering equality (2.21), the second equation of the system (2.20), and the first equation of the system (2.17). Considering the given (required) calculation accuracy, as a result, $C_{1/} \approx 229{,}34841$ m is obtained (Fig. 5), confirming that within the established

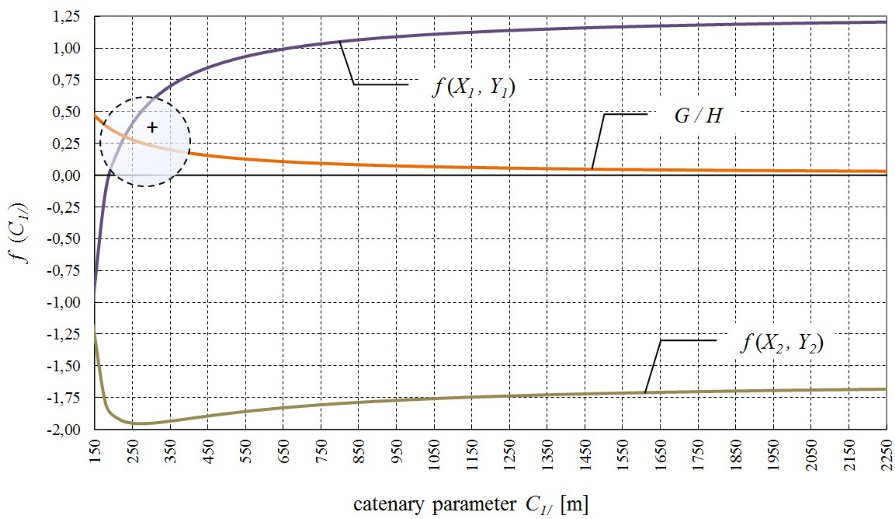

Fig. 5. Determination of the catenary parameter $C_{1/}$ using the computational algorithms of a spreadsheet processor (graphical-analytical method) and with the possibilities of further scaling.

limits of change for the specified parameter, the solution of the transcendental equation is unique.

In Fig. 5, the value Y_1 corresponds to the "+" sign in formula (2.19), and the value Y_2 corresponds to the "−" sign in the same formula. Accordingly, the values X_1 and X_2 are determined according to the first formula of the system of Eqs. (2.17) depending on the values of Y_1 and Y_2. Having established the catenary parameter $C_{1/}$, the other parameter and the remaining coefficients of the catenaries are determined from the transcendental equations constructed for this suspension engineering structure: according to formula (2.21) and Fig. 5, $C_{2//} \approx 63.11274$ m; the second formula (2.20) and Fig. 5, $C_{2/} \approx 131.21961$ m; formula (2.7) – $C_{1//} \approx 229.34841$ m; formula (2.3) – $C_{3/} \approx 267.92170$ m; formula (2.5) – $C_3^{//} \approx 253.76450$ m. In the process of stepwise finding the roots of the system of transcendental Eqs. (2.3)–(2.5), (2.7), (2.10) and (2.11), the correctness of the calculations is verified, taking into account the adopted calculation accuracy (Table 1).

Table 1. Verification of the correct calculation of coefficients (parameters) of catenaries as sag curves of the supporting element.

The serial number of the equation	The calculated value parts of the equation		Relative error [%]
	left	right	
(2.3)	1.16819...	1.16819...	< 0.001
(2.4)	1.58255...	1.58255...	< 0.001
(2.5)	−24.04113...	−24.04113...	< 0.001
(2.7)	229.34841...	229.34841...	< 0.001
(2.10)	0.30438...	0.30438...	< 0.001
(2.11)	350	350.00000...	< 0.001

Other geometric characteristics and force parameters of the suspension engineering structure are determined according to the following formulas: (2.24) – $x^*_{//} = 144.848$ m, (2.22) – $f_{\max} = 62.417$ m, (2.2) and (2.7) – $H = H_/ = H_{//} = 6570.832$ N, Fig. 4 – $T_{Ay} = 3967.931$ N, $T_{Cy\,left} = 2375.885$ N, $T_{Cy\,right} = 375.885$ N, $T_{By} = -8059.569$ N, (2.25) – $T_A = 7675.957$ N, $T_{C\,left} = 6987.178$ N, $T_{av/} = 7302.667$ N, (2.26) – $T_{C\,right} = 6581.575$ N, $T_B = 10398.677$ N, $T_{av//} = 7738.632$ N, (2.27) – $T_{av} = 7665.971$ N. For the purpose of visualizing the static position of the supporting element according to formulas (2.1), graphs of the corresponding functions are constructed, and the calculated above parameters are also indicated at the established scale (Fig. 6).

To investigate the possible change in geometric characteristics and force parameters of the aforementioned suspension structure depending on the change in the position of the point of application of the concentrated force G (point C),

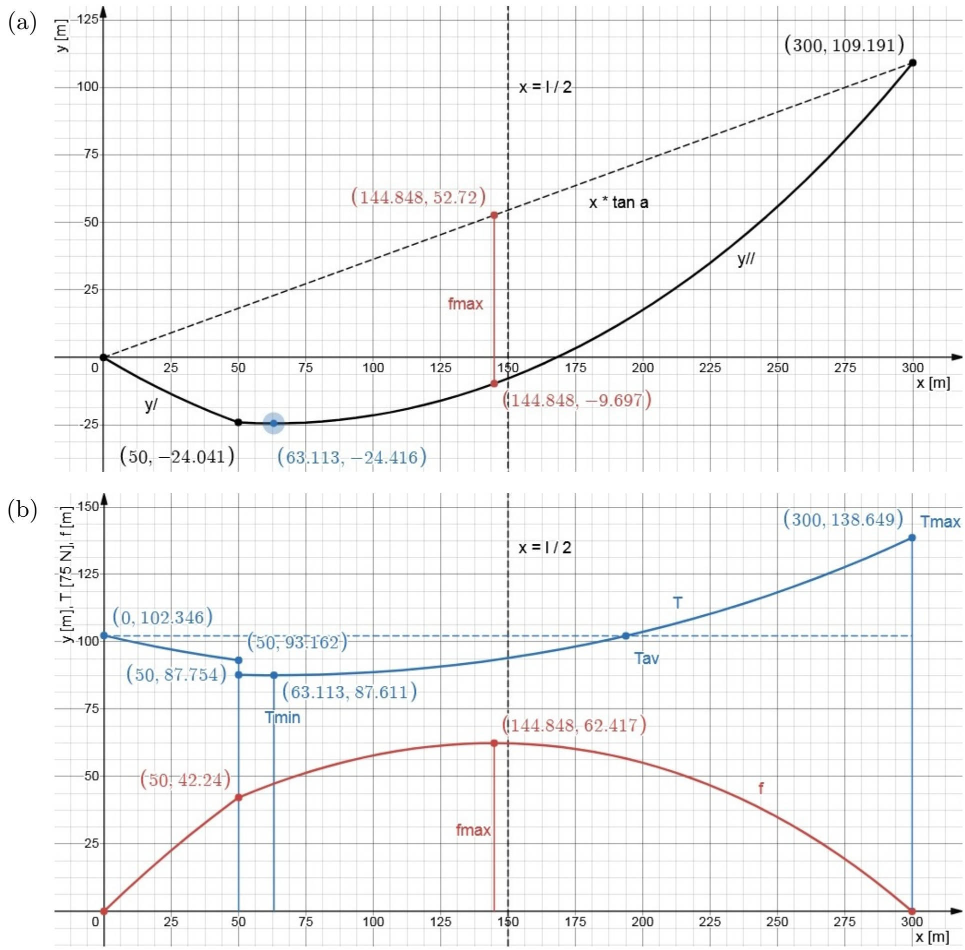

Fig. 6. Sag curves in the form of catenaries $y_{/}$ and $y_{//}$: (a) tension diagrams T and sag f, (b) of the flexible supporting element of a single-span suspension structure with span length $\ell = 300$ m.

a series of similar calculations (Figs. 7 and 8) are performed using a specialised applied computer program [23], gradually changing the value of x_C from 0 to 300 m with a step of $\Delta\ell = 10$ m (under the conditions $x_C = 0$ and $x_C = \ell$, the flexible element is under the load of its own weight only, and the load from the concentrated force G in this case is transmitted exclusively to the support).

Analysis of the obtained results (Figs. 7 and 8) allows for a preliminary assessment from an engineering perspective of the so-called "critical" location of the vertical concentrated force G within the span, where the sag and tension of the supporting element reach their maximum values (in this case, when the suspension structure is loaded with the force G at a distance of $x_C \approx 170$ m

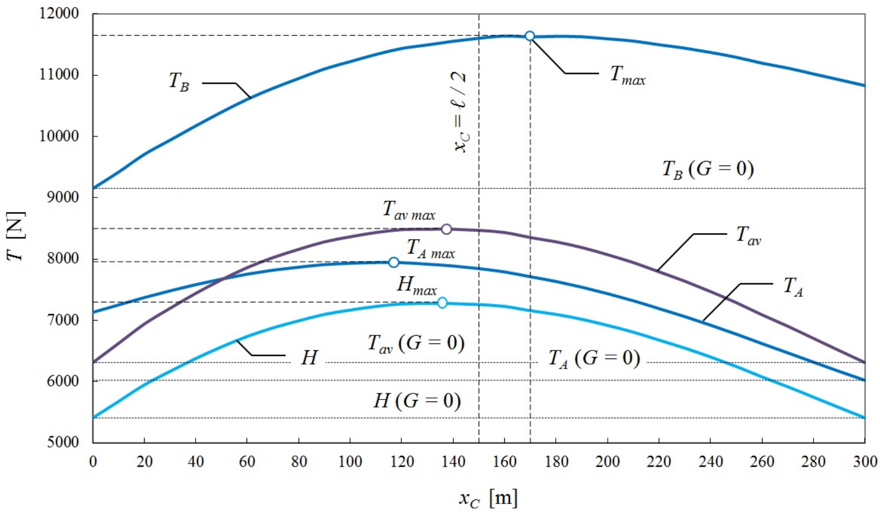

Fig. 7. Change in the components of the supporting element tension of the suspension structure at characteristic cross-sections depending on the abscissa x_C of the point of application of the vertical concentrated force G.

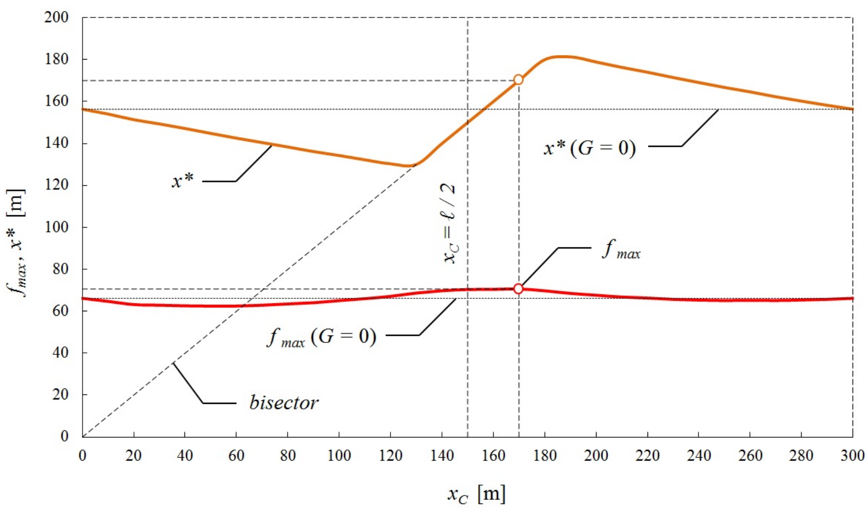

Fig. 8. Change in the position x^* and magnitude of the maximum sag of the supporting element $f_{\max}$ depending on the abscissa x_C of the point of application of the vertical concentrated force G.

from the lower support). It can be asserted that for an asymmetrically suspended supporting element, when the vertical concentrated force G is placed in the middle of the span (at $x_C = 0.5\ell$), none of the criterion functions (tensions and sags) reaches an extreme value, which is partially reflected in the studies [4, 9].

The adequacy of the proposed model was also assessed by comparing the theoretically calculated values of the two main parameters (tensions of the flexible element T and its sagging f) with the results of virtual simulation and using the finite element method in the software environment for engineering modeling and computer analysis Ansys (Fig. 9).

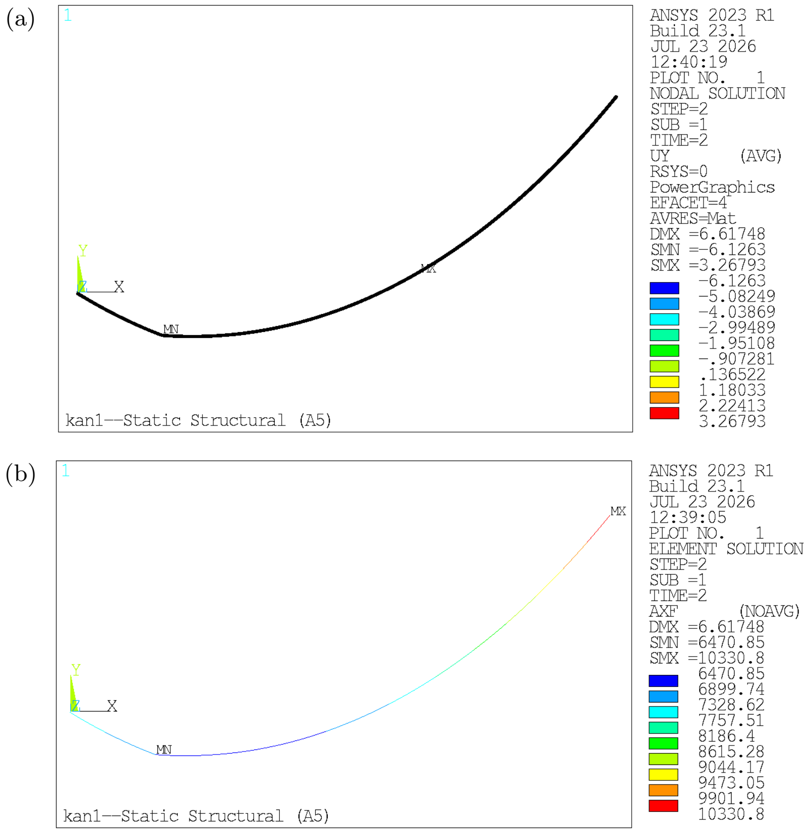

FIG. 9. Results of virtual simulation of sag curves: (a) and tension diagrams T, (b) of the flexible supporting element of a single-span suspension structure with span length $\ell = 300$ m in the Ansys Engineering Simulation Software environment.

The comparison of the obtained results (Fig. 10a, Fig. 11a) was performed according to absolute and relative errors (Fig. 10b, Fig. 11b), and the statistical significance of the differences was checked by calculating the Pearson correlation coefficient for $n = 31926$ experimental points for each of the two main parameters.

In the course of investigating changes in the tension of a flexible element T along the span using the proposed approach and the Ansys software environment

(Fig. 10), the absolute deviation lies within the range $-286.19152\ldots 79.36553$ N ($\Delta T_{\min}\ldots\Delta T_{\max}$), the mean absolute deviation $\Delta T_{av} = -87.63596N$, and the relative error is within the range $-4.10\ldots 1.21\%$ ($\delta_{\min}\ldots\delta_{\max}$), the mean relative error $\delta_{av} = -1.13\%$; parameters of the linear regression line: intercept $a = 46.03752$ N, slope $b = 0.98256$, Pearson's correlation coefficient $R^2 = 0.99884$.

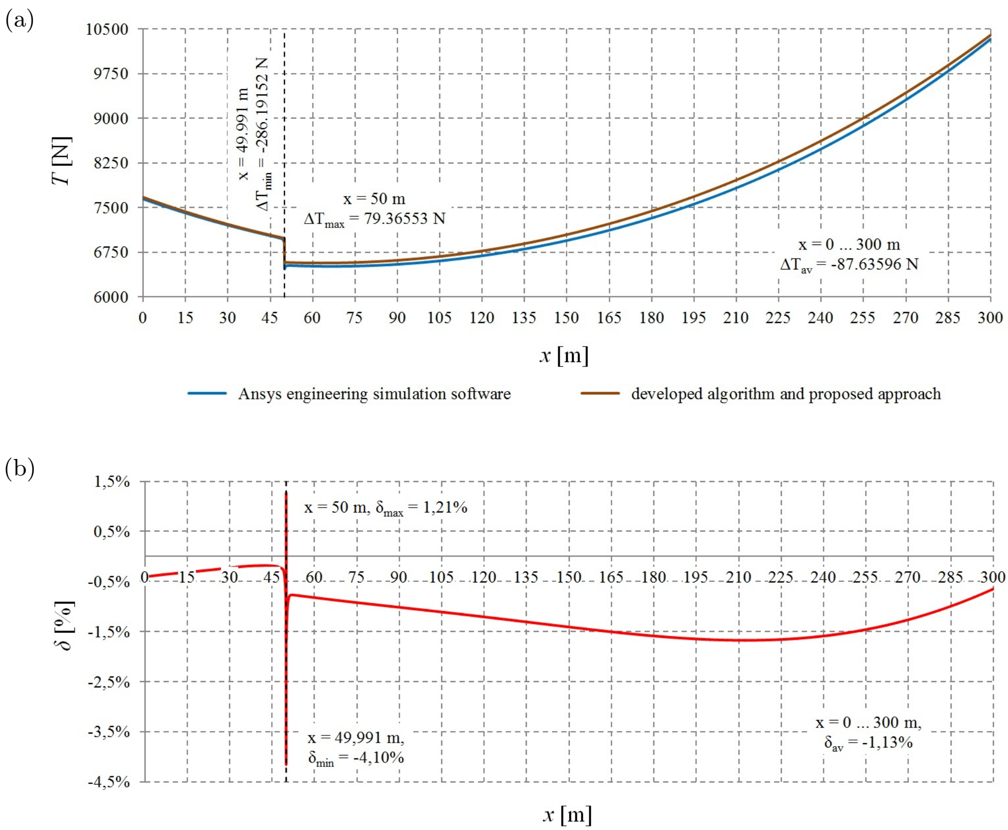

Fig. 10. Estimation of absolute errors ΔT: (a) and relative errors δ, (b) in determining the tension value of the flexible element T.

In the course of investigating changes in the sagging of a flexible element f along the span using the proposed approach and the Ansys software environment (Fig. 11), the absolute deviation lies within the range $-6.71775\ldots 5.54984$ m ($\Delta f_{\min}\ldots\Delta f_{\max}$), the mean absolute deviation $\Delta f_{av} = 1.33369$ m, and the relative error is within the range $-15.90\ldots 16.42\%$ ($\delta_{\min}\ldots\delta_{\max}$), the mean relative error $\delta_{av} = 2.72\%$; parameters of the linear regression line: intercept $a = -0.92031$ m, slope $b = 1.05224$, Pearson's correlation coefficient $R^2 = 0.96649$.

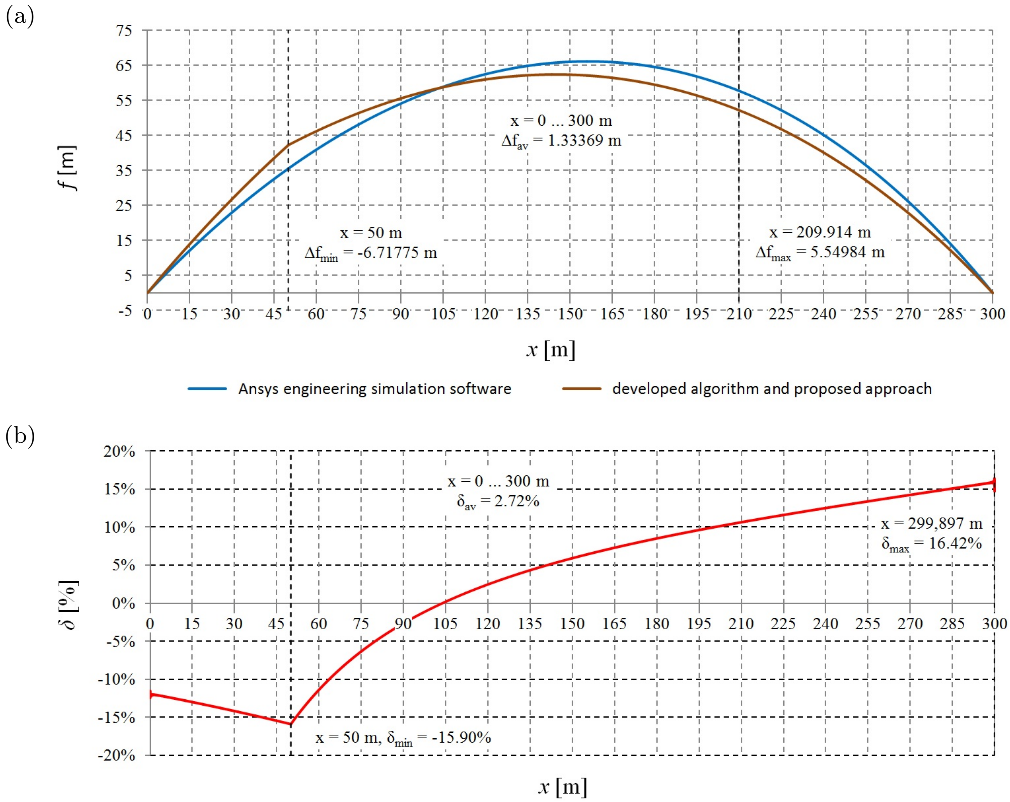

Fig. 11. Estimation of absolute errors Δf: (a) and relative errors δ, (b) in determining the sagging value of the flexible element f.

Given the values of the calculated accuracy and correlation metrics, it can be concluded that the model proposed in this paper is adequate, that it is physically sound, that the approach adopted is reasonable, and that the algorithm developed is correct.

4. Conclusions

The scientific article proposes a general approach to modelling and static analysis of a single-span suspension structure with an arbitrarily tensioned supporting element (rope, cable, chain, etc.), which is loaded by the combined action of uniformly distributed along the length and concentrated vertical loads. Using the theoretical foundations of the most accurate analytical catenary method available today and a continuous model of the flexible element, the shape of the sag curve has been established and an algorithm for calculating its geometric characteristics and force parameters has been developed by constructing and solving systems of transcendental equations. The development and the use of specialised computer software (based on the method of successive approximations) have been identified as a priority, considering the accuracy and labour intensity of solving these systems of equations. The article demonstrates that in the absence of modern specialised software complexes capable of solving systems of transcendental equations with many unknowns, researchers can obtain the necessary results (without loss of calculation accuracy, but with somewhat greater labour costs) by using the proposed analytical dependencies and computational algorithms of spreadsheet processors (based on the graphical-analytical method). The paper presents schematic diagrams of vertical load, tensions, and sag of the supporting element, as well as the results of numerical static analysis of the suspension structure (calculations performed using a specific example).

Overall, the obtained research results can be applied at the stage of engineering design of suspension structures in many fields of mechanical engineering and structural mechanics, as well as for improving existing applied calculation methods for flexible supporting elements. The presented theoretical developments regarding the modelling of suspension structures generally expand the scope of practical application of the catenary method and can be applied for calculating the design and operational parameters of engineering structures, machines, and industrial equipment equipped with a flexible supporting element (rope, cable, chain, etc.), which are loaded by concentrated and uniformly distributed vertical loads along their length (for example, self-weight, load weight, or other loads).

The novelty of this study lies in combining analytical and numerical treatment of suspension structures under vertical loading, with the development of a reduced transcendental formulation and practical computational algorithms that remain applicable even without specialised software. The proposed approach to modelling suspension structures, in addition to the input data presented in the article, allows for considering other additional factors in the future if necessary (for example, elastic and temperature deformations of the supporting element, an increase in the number of spans, compliance of end and intermediate supports, wind and snow-ice loads, etc.).

Acknowledgments

The work presented in this article was carried out as part of the research "Resource-efficient machinery and technologies for forest-based and agricultural production", the state registration number 0125U003986, Educational and Research Institute of Mechanical Engineering, Automation and Computer-Integrated Technologies, Ukrainian National Forestry University (Ukraine).

References

1. O. MOLOGNI, C.K. LYONS, G. ZAMBON, A.R. PROTO, G. ZIMBALATTI, R. CAVALLI, S. GRIGOLATO, *Skyline tensile force monitoring of mobile tower yarders operating in the Italian Alps*, European Journal of Forest Research, **138**, 5, 847–862, 2019, https://doi.org/10.1007/s10342-019-01207-0.

2. I. RUDKO, B. BAKAY, L.G. BONT, Y. ROMASEVYCH, S. HORZOV, *Calculation of optimal length for skyline*, Bulletin of the Transilvania University of Brasov, Series II: Forestry, Wood Industry, Agricultural Food Engineering, **15**, 1, 79–90, 2022, https://doi.org/10.31926/but.fwiafe.2022.15.64.1.6.

3. M. MARTYNCIV, B. SOLOHUB, M. MATIISHYN, *Dynamics and Reliability of Suspended Rope Systems*, Monograph, Lviv Polytechnic University Press, Lviv, 2011 [in Ukrainian].

4. J. SESSIONS, K. LYONS, J. WIMER, *Maximizing the standing skyline log load using a variable length tagline*, Forests, **12**, 7, 927, 2021, https://doi.org/10.3390/f12070927.

5. V.K. BAY, D.V. TAI, D.V. NGOC, L.A. TUAN, H. NHAN, H. HA, *Calculation method for elastic parabolic cable subjected to uniformly distributed load on each segment and concentrated load at many point*, Engineering Solid Mechanics, **11**, 4, 353–368, 2023, https://doi.org/10.5267/j.esm.2023.5.008.

6. L.G. BONT, L. RAMSTEIN, F. FRUTIG, J. SCHWEIER, *Tensile forces and deflections on skylines of cable yarders: Comparison of measurements with close-to-catenary predictions*, International Journal of Forest Engineering, **33**, 3, 195–216, 2022, https://doi.org/10.1080/14942119.2022.2051159.

7. J. QIN, J. CHEN, L. QIAO, J. WAN, Y. XIA, *Catenary analysis and calculation method of track rope of cargo cableway with multiple loads*, MATEC Web of Conferences, EDP Sciences, **82**, 01008, 1–7, 2016, https://doi.org/10.1051/matecconf/20168201008.

8. I. ORYNYAK, F. GUARRACINO, M. MODANO, R. MAZURYK, *An efficient iteration procedure for form finding of slack cables under concentrated forces*, Archives of Civil Engineering, **68**, 2, 645–663, 2022, https://doi.org/10.24425/ace.2022.140664.

9. A. HATIBOVIC, *Derivation of equations for conductor and sag curves of an overhead line based on a given catenary constant*, Periodica Polytechnica Electrical Engineering and Computer Science, **58**, 1, 23–27, 2014, https://doi.org/10.3311/PPee.6993.

10. J.B. LI, G.B. ZHU, Z.S. OU, *The method to calculate the length of the catenary for anchored vessel*, Applied Mechanics and Materials, **624**, 356–360, 2014, https://doi.org/10.4028/www.scientific.net/AMM.624.356.

11. H.M. IRVINE, G.B. SINCLAIR, *The suspended elastic cable under the action of concentrated vertical loads*, International Journal of Solids and Structures, **12**, 4, 309–317, 1976, https://doi.org/10.1016/0020-7683(76)90080-9.

12. J. BENET, F. CUARTERO, T. ROJO, P. TENDERO, E. ARIAS, *Numerical algorithms for the analysis of initial configuration in a railway catenary structure and its code implementation: a software tool CALPE*, Mathematical Problems in Engineering, **2015**, 1, 819165, 1–16, 2015, https://doi.org/10.1155/2015/819165.

13. A. LUONGO, D. ZULLI, *Static perturbation analysis of inclined shallow elastic cables under general 3D-loads*, Curved and Layered Structures, **5**, 1, 250–259, 2016, https://doi.org/10.1515/cls-2018-0018.

14. A. Luongo, D. Zulli, *Statics of shallow inclined elastic cables under general vertical loads: A perturbation approach*, Mathematics, **6**, 2, 24, 2018, https://doi.org/10.3390/math6020024.

15. M. Lepidi, *Catenary configuration and geometric stiffness matrix of inextensible cables: Analytical high-order asymptotic solutions for parametric design*, Applied Mathematical Modelling, **128**, 1–25, 2024, https://doi.org/10.1016/j.apm.2023.12.019.

16. M. Lepidi, *Free vibrations of shallow inextensible cables: a perturbation approach*, Nonlinear Dynamics, **113**, 22, 30443–30472, 2025, https://doi.org/10.1007/s11071-024-10536-8.

17. S. Corazza, F. Foti, V. Denoël, *Asymptotic solutions for the modal properties of shallow cables with small bending stiffness and compliant supports*, Applied Mathematical Modelling, **161**, 117156, 2027, https://doi.org/10.1016/j.apm.2026.117156.

18. H. Mouradi, A. El Barkany, A. El Biyaali, *Steel wire ropes failure analysis: Experimental study*, Engineering Failure Analysis, **91**, 234–242, 2018, https://doi.org/10.1016/j.engfailanal.2018.04.019.

19. W. Cecot, S. Milewski, J. Orkisz, *Determination of overhead power line cables configuration by FEM and meshless FDM*, International Journal of Computational Methods, **15**, 02, 1850004, 1–20, 2018, https://doi.org/10.1142/S0219876218500044.

20. L. Greco, N. Impollonia, M. Cuomo, *A procedure for the static analysis of cable structures following elastic catenary theory*, International Journal of Solids and Structures, **51**, 7-8, 1521–1533, 2014, https://doi.org/10.1016/j.ijsolstr.2014.01.001.

21. M. Such, J.R. Jimenez-Octavio, A. Carnicero, O. Lopez-Garcia, *An approach based on the catenary equation to deal with static analysis of three dimensional cable structures*, Engineering Structures, **31**, 9, 2162–2170, 2009, https://doi.org/10.1016/j.engstruct.2009.03.018.

22. I. Rudko, B. Bakay, A.E. Akay, V. Loveikin, Y. Romasevych, *Static analysis of suspension systems with uniformly distributed vertical load*, Journal of Theoretical and Applied Mechanics, **55**, 1, 105–119, 2025, https://doi.org/10.55787/jtams.25.55.1.105.

23. I. Rudko, V. Baryliak, V. Matushevsky, *Computer programme "Designing routes for suspended cableways for forestry purposes based on single-span installations" ("Route FI SCW 1")*, Certificate No. 57762 dated 22.12.2014, Bulletin "Copyright and Related Rights", No. 35, dated 30.01.2015, https://iprop-ua.com/cr/0a5uyt40.

Received April 10, 2026; revised version July 31, 2026.
Published online September 14, 2026.